

Cationic Rhodium (I) Complexes of *N*-Phosphino-*tert*-butylsulfonamide Ligands: Synthesis, Structure, and Coordination Modes

Thierry Achard, Jordi Benet-Buchholz, Antoni Riera,* and Xavier Verdaguer*

Unitat de Recerca en Síntesi Asimètrica (URSA-PCB), Institute for Research in Biomedicine (IRB Barcelona) and Departament de Química Orgànica, Universitat de Barcelona, c/Baldiri Reixac 10, E-08028 Barcelona, Spain, and Institute of Chemical Research of Catalonia (ICIQ), Avda. Països Catalans 16, 43007 Tarragona, Spain

Received July 18, 2008

Here we describe the rhodium (I) complexes of *N*-phosphino-*tert*-butylsulfonamide ligands. This novel class of hemilabile ligands (PNSO) can work as either P,O or P,S chelating ligands when attached to the square planar rhodium center. Complexes bearing diene ligands such as [Rh(PNSO)(NBD)][TfO] and [Rh(PNSO)(COD)][TfO] provided P,O coordination, whereas [Rh(PNSO)₂][TfO]-type complexes provided P,S coordination. Ligand exchange experiments with mono and bidentate phosphines afforded evidence of the hemilabile behavior of the PNSO ligands.

Introduction

Bidentate ligands have become the most powerful tool in metal-catalyzed asymmetric processes.¹ Chelation provides the rigidity required to firmly allocate the chiral information around the metal center. Usually, the chirality of these ligands resides in the carbon backbone; however, some have a chiral phosphorus or sulfur center. The synthesis of chiral-phosphorus compounds is complex and difficult. Conversely, chiral-sulfur compounds can be prepared efficiently, and some are commercially available in large scale.^{2–5} Our group has recently reported *N*-phosphino-*tert*-butylsulfonamides (I) as new class of chiral bidentate ligands (PNSO) and their application in the intermolecular asymmetric Pauson-Khand reaction.⁶ In response to dicobalt carbonyl complexes, the PNSO ligand acts as a hemilabile bridging P,S ligand, thereby providing type II complexes (Figure 1).

An essential feature of hemilabile ligands is the presence of at least one labile donor function while the other donor group remains firmly bound to the metal center(s). Hemilabile ligands have the capacity to provide open coordination sites at the metal center during reactions that are “masked” in the ground-state structure and to stabilize reactive intermediates.⁷ PNSO ligands are an unusual class of hemilabile ligands, since the sulfoxide moiety can bind the metal through either sulfur or oxygen, thus enabling the ligand to provide both P,S and P,O chelation (Scheme 1). We have previously shown that PNSO ligands work solely as P,S bridging ligands toward bimetallic cobalt–carbonyl complexes; however, there is no data on the coordination

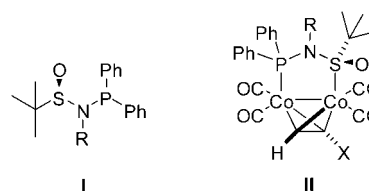
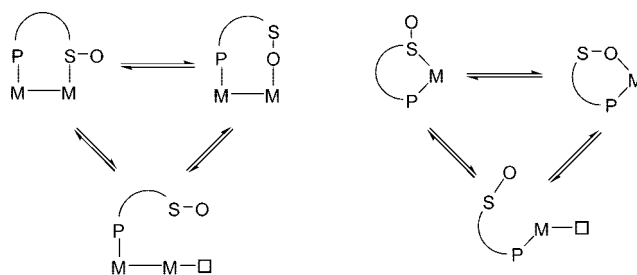


Figure 1

Scheme 1. Possible Coordination Modes of *N*-Phosphino Sulfonamide Ligands with Mono- and Bimetallic Complexes



behavior of these ligands toward monometallic systems. Here, we report on the cationic rhodium (I) complexes of *N*-benzyl-*N*-phosphino-*tert*-butylsulfonamide ligands, their structure, coordination modes, and their behavior toward ligand exchange reactions.

Results and Discussion

Synthesis of the Ligands. Chiral PNSO ligands were synthesized from the commercially available *tert*-butylsulfonamide (+)-**1** (Scheme 2). The synthesis of **1** in two steps from the inexpensive starting material *tert*-butyl disulfide has been reported by Ellman and co-workers.⁸ From (+)-**1**, reductive amination protocol with Ti(OEt)₄ in the presence of benzaldehyde produced an intermediate sulfinimine, which was reduced in situ to the corresponding sulfonamide (**2**).⁹ In an optimized

* Corresponding author. E-mail: xavier.verdaguer@irbbarcelona.org.

(1) Jacobsen, E. N.; Pfaltz, A.; Yamamoto, H. In *Comprehensive Asymmetric Catalysis*; Springer: Berlin, 1999; Vol. I–III.

(2) Fernandez, I.; Khair, N. *Chem. Rev.* **2003**, *103*, 3651–3706.

(3) Pellissier, H. *Tetrahedron* **2006**, *62*, 5559–5601.

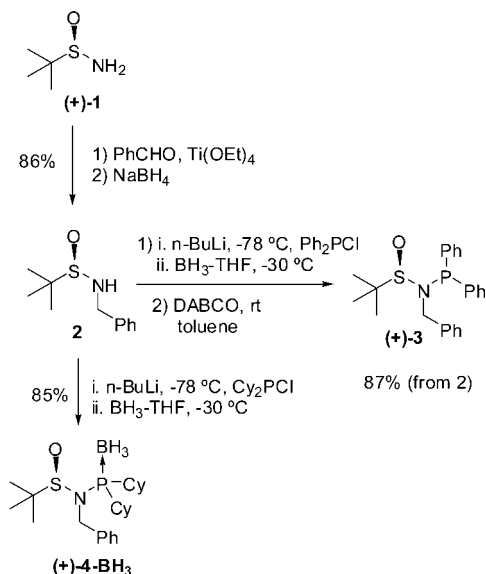
(4) Senanayake, C. H.; Krishnamurthy, D.; Lu, Z.; Han, Z.; Gallou, I. *Aldrichim. Acta* **2005**, *38*, 93–104.

(5) Mellah, M.; Voituriez, A.; Schulz, E. *Chem. Rev.* **2007**, *107*, 5133–5209.

(6) Solà, J.; Revés, M.; Riera, A.; Verdaguer, X. *Angew. Chem., Int. Ed.* **2007**, *46*, 5020–5023. Revés, M.; Achard, T.; Solà, J.; Riera, A.; Verdaguer, X. *J. Org. Chem.* **2008**, *73*, 7080–7087.

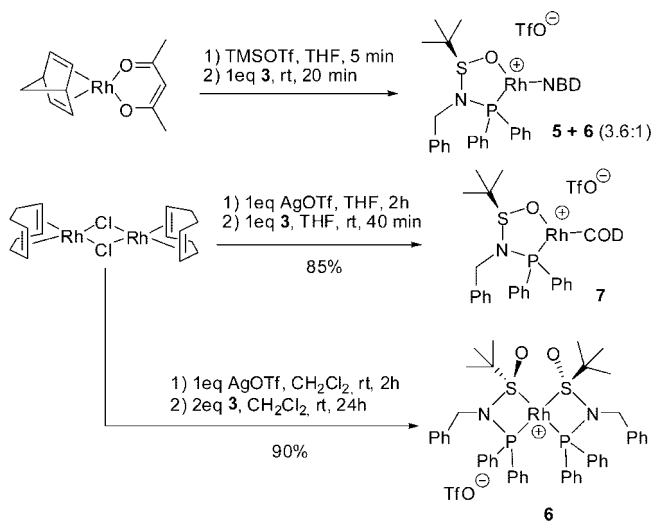
(7) Braunstein, P.; Naud, F. *Angew. Chem., Int. Ed.* **2001**, *40*, 680–699.

(8) Cogan, D. A.; Liu, G.; Kim, K.; Backes, B. J.; Ellman, J. A. *J. Am. Chem. Soc.* **1998**, *120*, 8011–8019.

Scheme 2. Synthesis of Optically Pure *N*-Phosphino-*N*-benzyl-*tert*-butylsulfonamide Ligands

protocol, anion formation with *n*-BuLi at low temperature followed by the addition of either Ph₂PCl or Cy₂PCl and protection of the phosphine moiety with borane provided the corresponding borane-protected ligands **3**-BH₃ and **4**-BH₃ (Scheme 2). In the case of diphenylphosphine, the borane-free ligand was obtained by deprotection with DABCO at room temperature to afford (+)-**3** as a crystalline solid in good yield. Conversely, borane-free ligand **4** could not be isolated because of the undesired sulfur-to-oxygen migration that leads to the corresponding phosphine oxide.^{10,11} Therefore, the cyclohexylphosphine ligand was used in its borane-protected form, **4**-BH₃, throughout the present study.

***N*-Benzyl-*N*-diphenylphosphino-*tert*-butylsulfonamide (3): Synthesis and Characterization of Its Cationic Rhodium Complexes.** The first attempts to obtain a cationic Rh complex with ligand **3** followed the procedure described by Alcock and co-workers, who reported the synthesis of a phosphine sulfoxide ligand and its Rh^I-NBD complex.¹² In that study, Alcock used (NBD)Rh(acac) as the rhodium source and TMSOTf to remove the acac ligand from the metal. Following this procedure, we treated a solution of (NBD)Rh(acac) in dry THF at room temperature under N₂ with 1 equiv of TMSOTf, followed by 1 equiv of ligand **3** (Scheme 3). After 20 min at room temperature, the mixture was added to a vigorously stirred hexane solution to give a yellow precipitate. ¹H NMR (CDCl₃) of this solid showed both noncoordinated and metal-coordinated NBD and no trace of the corresponding original ligand (*t*-Bu, 0.93 ppm). Two new major metal species were present with resonances at 1.47 and 1.34 ppm for the *t*-Bu group. Consistently, ³¹P NMR showed two doublets at 69.5 and 115.8 ppm, respectively, with a phosphorus–rhodium coupling constant of 141 and 193 Hz, respectively. This mixture was crystallized upon layering a hexane/Et₂O mixture over CH₂Cl₂. This approach produced a few dark orange crystals suitable for X-ray

Scheme 3. Synthesis of Cationic Rhodium (I) Complexes with Ligand 3

analysis. The crystalline compound (**5**) was the corresponding (PNSO)Rh^I(NBD) triflate complex with the PNSO ligand acting as a bidentate P,O ligand (Figure 2). ¹H NMR of pure **5** shows resonances at 1.34 ppm for the *t*-Bu group and two low-field broad doublets for the benzylic PhCH₂N protons at 4.47 and 4.58 ppm. The metal coordinated NBD showed the olefinic protons as a broad resonance centered at 4–5 ppm. Unfortunately, we could obtain only small amounts of pure **5** with this methodology, and its preparation was not consistently reproducible. In addition to this, compound **5** showed limited stability in solution.

Alternatively, the analogous (PNSO)Rh^I(COD) complex was prepared in good yield (85%) using [RhCl(COD)]₂ as a metal source (Scheme 3). Thus, chloride abstraction with AgOTf in dry THF and addition of ligand **3** under N₂ provided the desired compound (**7**) after 40 min at room temperature. This compound was isolated as an air-stable orange solid by layering the reaction mixture with diethyl ether. ¹H NMR of **7** showed the *t*-Bu resonance at 1.54 ppm in CDCl₃ and four signals corresponding to the olefinic protons of the metal-coordinated COD ligand, as would be expected for a complex with no symmetry. Suitable crystals for X-ray analysis were obtained by slow diffusion of Et₂O into a CH₂Cl₂ solution of **7**. The resulting structure revealed that **3** again acts as a P,O bidentate ligand (Figure 2), in analogy to the structure of complex **5**.

Metal–phosphorus and metal–oxygen, as well as oxygen–sulfur distances for **5** and **7** are consistent with the structure of [Ph₂PCH₂S(O)Ph]Rh^I(NBD) reported by Alcock and co-workers (Figure 2).¹² The Rh–O–S–N–P atoms formed a five-member ring with an envelope-like conformation in which the oxygen bonded to rhodium was slightly out of plane (0.44 Å). This observation differs from the structure reported by Alcock, in which it is the central carbon atom of the ligand that is out of plane. A strong trans effect was observed for both structures on the Rh–olefin distances. For example, **5** showed Rh–C (olefinic) distance trans to phosphorus of 2.231(2) and 2.237(2), whereas the Rh–C (olefinic) distance trans to oxygen was 2.093(1) and 2.093(2). The olefinic group placed trans to the most electronegative donor atom presented a shorter and stronger bond to the metal. Alignment of structures **5** and **7** without the olefinic ligands produced an almost perfect fit, except for the *N*-benzyl group (Figure 3). In complex **5**, the benzyl group was perpendicular to the phenyl ring of the phosphine, whereas in complex **7**, it showed a parallel-type disposition. The observed

(9) Tanuwidjaja, J.; Peltier, H. M.; Ellman, J. A. *J. Org. Chem.* **2007**, *72*, 626–629.

(10) Hiroi, K.; Suzuki, Y.; Kawagishi, R. *Tetrahedron Lett.* **1999**, *40*, 715–718.

(11) Vedejs, E.; Meier, G. P.; Powell, D. W.; Mastalerz, H. *J. Org. Chem.* **1981**, *46*, 5253–5254.

(12) Alcock, N. W.; Brown, J. M.; Evans, P. L. *J. Organomet. Chem.* **1988**, *356*, 233–247.

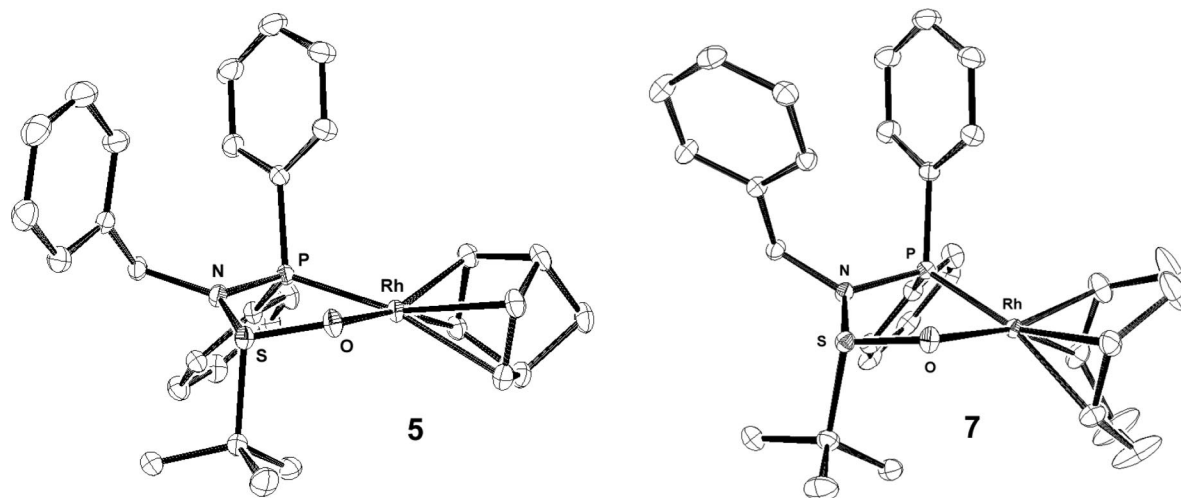


Figure 2. Ortep plot for crystal structures **5** and **7** with thermal ellipsoids shown at 50% probability. Only the metal cations are shown. For **5**, a single molecule of the two independent complexes that form the original unit cell is shown. Selected bond distances (Å) for **5** and **7**, respectively: Rh–O, 2.116(1) and 2.100(1); Rh–P, 2.262(1) and 2.250(1); S–O, 1.527(1) and 1.523(1).

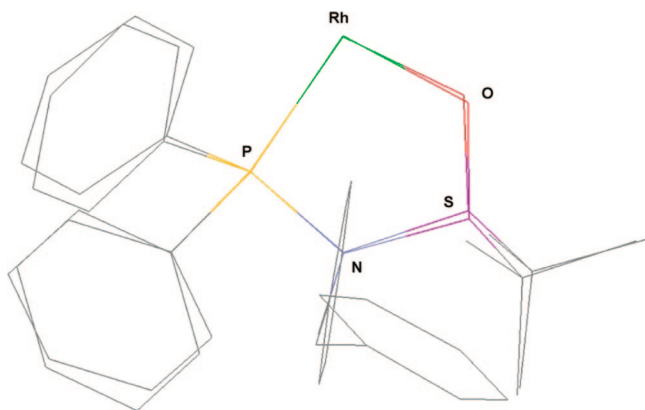


Figure 3. Alignment of Rh–P–N centers for complexes **5** and **7**. NBD and COD ligands are omitted for clarity.

O-bonding mode to the metal led to a considerable lengthening of the S=O bond (1.527(1) and 1.523(1) Å for **5** and **7**, respectively) in comparison with noncoordinated DMSO 1.493(av) Å. O-Coordination could, in principle, be expected in response to a hard cationic-Rh^I center. ³¹P NMR spectra of complexes **5** and **7** showed resonances at 115.8 and 116.5 ppm, respectively, whereas the free ligand **3** displayed the corresponding resonance at 60.0 ppm. In addition, Milstein and co-workers reported a [Rh(COD)(DMSO)₂][BF₄] complex in which both DMSO molecules bind the metal through oxygen.¹³ These findings indicate that the presence of a diolefinic ligand on the metal makes this center more electron-deficient, thereby favoring the O-coordination mode of the PNSO ligand.

We next examined the preparation of rhodium species with two PNSO ligands. With this purpose, [RhCl(COD)]₂ was treated with AgOTf in dichloromethane, and the resulting solution was added to a solution of 2 equiv of ligand **3** and stirred for 24 h at room temperature (Scheme 3). The resulting yellow mixture was poured over stirred Et₂O to provide an air-stable yellow precipitate. Spectroscopic analysis of this solid revealed the presence of a single substance with ¹H NMR resonances at 1.47 ppm (*t*-Bu). ³¹P NMR showed a doublet at 69.5 ppm and coupling constant of 141 Hz, which corresponded

to one of the substances obtained in the initial experiments with (NBD)Rh(acac). Finally, ESI mass spectroscopy confirmed the new substance (**6**) as a *bis*-(PNSO) rhodium (I) triflate. Traditionally, IR spectroscopy is a good tool to distinguish whether O–M or S–M bonding occurs in sulfoxide metal complexes.¹⁴ In our case, although noncoordinated **3** displayed an intense S=O absorption band at 1074 cm^{−1}, no diagnostic bands were observed for complexes **5**, **6**, or **7**.

To elucidate the structure of the dimeric PNSO complex and the coordination mode of the sulfonamide moiety, single crystals for X-ray analysis were obtained by layering Et₂O over a CH₂Cl₂ solution of **6** (Figure 4). The Rh center presented a slightly distorted square-planar geometry, with the two phosphorus atoms (and sulfur) in a *cis* arrangement in close analogy with other reported P–S, P–N, or P–O ligands.^{15–18} The Rh, S, N, and P atoms adopted a planar double diamond disposition in which the metal center was the connection point of two identical four-member rings. The complex showed a C₂ symmetry axis in the coordination plane of the metal. The oxygen atoms and the *t*-Bu groups of the sulfonamide were in anti position to each other to minimize steric and electronic interactions. The PNSO ligand provided bite angle (P–Rh–S) values of 71.33(2) and 71.20(2)°, which fall between dppm (70.80°) and MiniPHOS (72.96°) ligands in analogous Rh^I complexes.^{19,20} The Rh–P (2.251(1) and 2.249(1) Å) and Rh–S (2.289(1) and 2.288(1) Å) distances were quite similar. In this respect, the Rh–S distances observed were in the long range for an S-bonding mode.^{13,14,21} This observation could be attributed to the strong trans effect exerted by the phosphine ligands. Moreover, the occurrence of S-bonding in complex **6** can be reasoned on the

(14) Calligaris, M. *Coord. Chem. Rev.* **2004**, *248*, 351–375.

(15) Dick, D. G.; Stephan, D. W. *Can. J. Chem.* **1986**, *64*, 1870–1875.

(16) Esquiús, G.; Pons, J.; Yanez, R.; Ros, J.; Mathieu, R.; Donnadieu, B.; Lukan, N. *Eur. J. Inorg. Chem.* **2002**, 299, 9–3006.

(17) Kuznetsov, V. F.; Facey, G. A.; Yap, G. P. A.; Alper, H. *Organometallics* **1999**, *18*, 4706–4711.

(18) Braunstein, P.; Chauvin, Y.; Naehring, J.; DeCian, A.; Fischer, J.; Tiripicchio, A.; Ugozzoli, F. *Organometallics* **1996**, *15*, 5551–5567.

(19) Gridnev, I. D.; Yamanoi, Y.; Higashi, N.; Tsuruta, H.; Yasutake, M.; Imamoto, T. *Adv. Synth. Catal.* **2001**, *343*, 118–136.

(20) Fornika, R.; Six, C.; Gorls, H.; Kessler, M.; Kruger, C.; Leitner, W. *Can. J. Chem.* **2001**, *79*, 642–648.

(21) For the structure of a related neutral sulfonamide Rh(I) (COD) complex displaying sulfur coordination, see: (a) Souers, A. J.; Owens, T. D.; Oliver, A. G.; Hollander, F. J.; Ellman, J. A. *Inorg. Chem.* **2001**, *40*, 5299–5301.

(13) Dorta, R.; Rozenberg, H.; Shimon, L. J. W.; Milstein, D. *Chem.–Eur. J.* **2003**, *9*, 5237–5249.

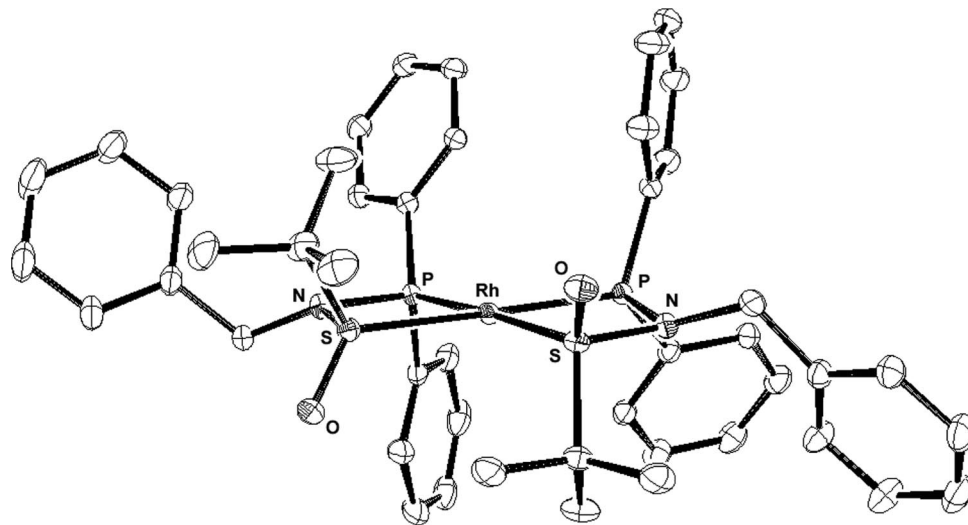
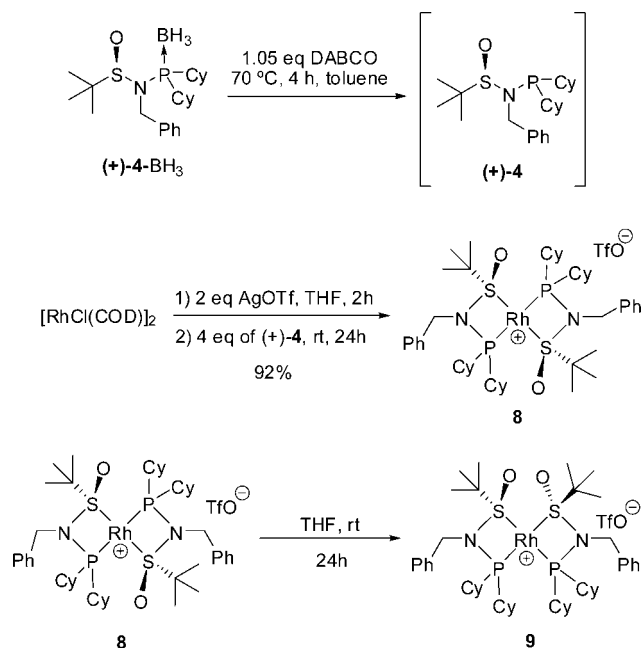


Figure 4. Ortep plot for crystal structure **6** with thermal ellipsoids shown at 50% probability. Only the metal cation is shown. Selected bond distances (Å) and angles (deg): Rh–P, 2.251(1) and 2.249(1); Rh–S, 2.289(1) and 2.288(1); P–Rh–S, 71.33(2) and 71.20(2).

Scheme 4. Synthesis of Cationic Rhodium Complexes with Ligand 4



basis that the metal center, which lacks the bis-olefin ligand, is more electron-rich than complexes **5** and **7** and thus prefers the softer S-coordination mode. This notion is corroborated by the ^{31}P NMR of complex **6** (69.5 ppm), which is very close to that of the free ligand **3** (60.0 ppm).

N-Benzyl-N-dicyclohexylphosphino-tert-butylsulfonamide (4): Synthesis and Characterization of Its Cationic Rh Complexes. The use of ligand **4** in the preparation of rhodium complexes presented an additional challenge; that is, it could not be isolated pure in its borane-free form. Deprotection of borane-protected PNSO ligands occurs in toluene in the presence of DABCO. Under these conditions in the presence of a base and prior to purification, the ligand preserves its integrity, as determined by ^1H and ^{31}P NMR (Scheme 4). Under these circumstances, we attempted the synthesis of the corresponding bis-PNSO–Rh^I complex. Thus, chloride removal on $[\text{RhCl}(\text{COD})]_2$ with AgOTf, an addition of the resulting solution to deprotected **4**, was left to stir for 24 h at room temperature.

The product was purified by flash chromatography of the reaction mixture on SiO_2 using hexane/acetone mixtures as mobile phase. This approach provided the desired bis PNSO complex **8** in an excellent 92% yield. ^1H NMR revealed a single *t*-Bu resonance at 1.46 ppm and for the benzylic PhCH_2N an AB system coupled to phosphorus at 4.29 and 4.46 ppm. The ^{31}P NMR spectrum displayed a single doublet at 86 ppm with a coupling constant to Rh of 121 Hz. ESI mass spectroscopy confirmed complex **8** as a bis-PNSO–rhodium complex. Again, no concluding information on the coordination mode of the sulfoxide fragment could be drawn from the IR spectra of **8**. Finally, crystallization of **8** in a hexane/THF mixture provided green-yellow plated crystals suitable for X-Ray analysis (Figure 5). In contrast to what we expected, complex **8** showed a trans configuration of the two phosphines and the two sulfonamide groups around the square planar rhodium center. The complex now showed a C_2 axis perpendicular to the Rh coordination plane. This configuration positioned the two *t*-Bu groups on the same face of the complex and caused a distortion of the square planar geometry around the metal. Thus, the P–Rh–P angle was $165.28(1)^\circ$, whereas the analogous S–Rh–S angle was $167.97(1)^\circ$. Longer Rh–P distances were observed (2.312(1) and 2.297(1) Å) for **8** because of the dicyclohexylphosphine residue's being a weaker back-bonding ligand than diphenylphosphine. Like complex **6**, double S-coordination mode was observed for the sulfonamide fragment. The Rh–S distances were 2.251(1) and 2.269(1) Å, again falling in the long-range for this type of bonding. This distance is in agreement with the trans S-bonded DMSO molecules in rhodium complexes reported by Milstein and co-workers and can be explained on the basis that S-bound sulfoxides have a relatively higher trans influence than O-bound sulfoxides.^{13,22}

After some experimentation, we observed that the bis-PNSO–Rh complex **8** was not configurationally stable. Solving **8** in THF provided a distinct PNSO complex. ^1H NMR analysis of the new complex **9** showed a *t*-Bu resonance at 1.63 ppm, and in the benzylic region, the original AB system for **8** changed to a multiplet. Additionally, a new doublet at 95 ppm and $J_{\text{Rh}} = 132$ Hz was observed in the ^{31}P NMR spectrum. Compound **9** crystallized as air-stable yellow needles (THF/hexanes). High-resolution mass spectroscopy (ESI) revealed a composition

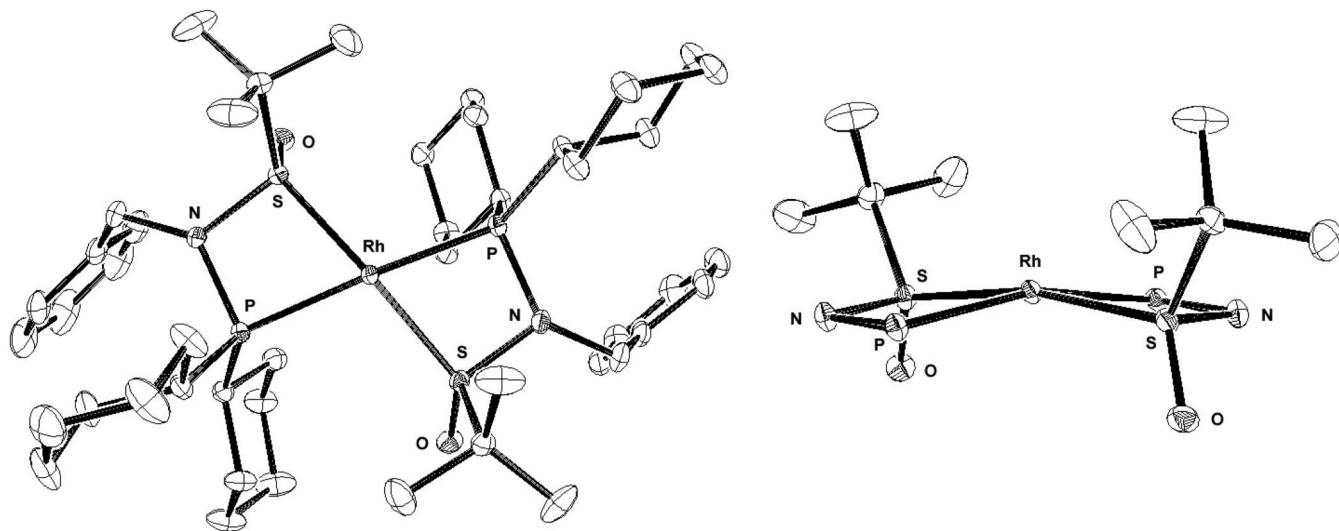
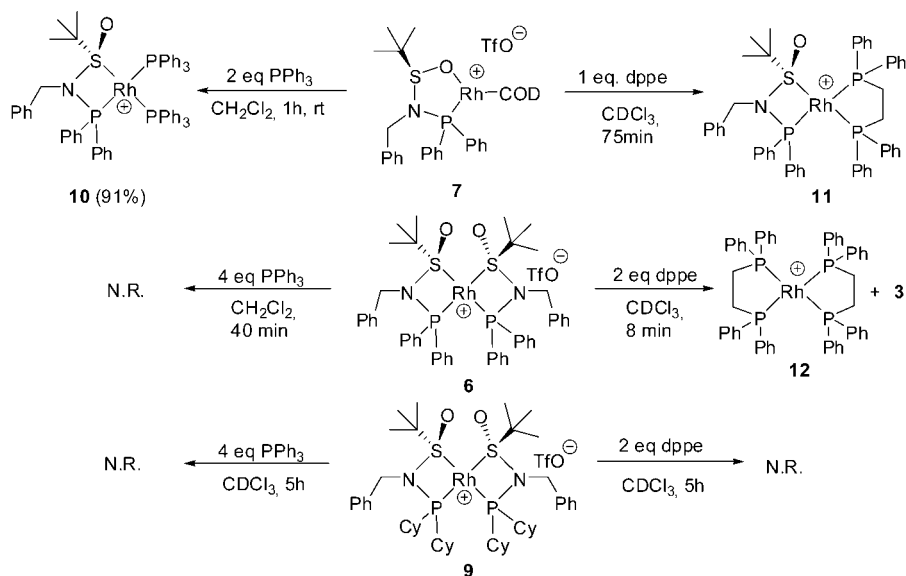


Figure 5. Ortep plot for crystal structure **8** with thermal ellipsoids shown at 50% probability (left). Lateral view of the central coordination core (right). Cyclohexyl and benzyl groups are omitted for clarity. Only the metal cation is shown. Selected bond distances (Å) and angles (deg): Rh–P, 2.312(1) and 2.297(1); Rh–S, 2.251(1) and 2.269(1); P–Rh–P, 165.28(1); S–Rh–S, 167.97(1).

Scheme 5. Reactivity of Rhodium (I) Complexes with Phosphines



identical to that of **8**. Solving **8** in a coordinating solvent such as THF (24 h) and acetonitrile (24 h) provided full conversion to the new complex **9** (Scheme 4). However, no isomerization from **8** to **9** was observed in CDCl₃ or toluene for 24 h. Moreover, the isomerization was not reversible, even when solving **9** in a nonpolar solvent for a long period of time (i.e., toluene). These experimental observations indicated that complex **8** is a kinetic product and **9** is the thermodynamically more stable complex. From the electronic point of view, the similarity of the ³¹P NMR resonances for **8** and **9** suggests that both are S-bonded complexes. All things considered, the proposed structure for complex **9** is the corresponding S-coordinated cis analog of **8** (Scheme 4). The cis configuration should be the thermodynamically preferred one. In structure **9** the *t*-Bu groups are placed at opposite faces of the complex, thus releasing the steric strain built up in **8** that resulted in a distortion of the square planar geometry.

Reactivity of Rhodium (I) Complexes with Phosphines.

To examine how competent the PNSO ligands were with respect to other phosphines, ligand exchange reactions with PPh₃ and dppe were carried out and monitored by ³¹P NMR (Scheme 5).

Reaction of [Rh(PNSO)(COD)][TfO] (**7**) with two equivalents of PPh₃ provided the corresponding [Rh(PNSO)(PPh₃)₂][TfO] complex **10**, which was synthesized and isolated in an excellent 91% yield in preparative scale. Compound **10** showed the characteristic pattern for three nonequivalent phosphorus atoms attached to a square-planar Rh center in the ³¹P NMR: three resonances with three distinct couplings each, two couplings to phosphorus, and one to rhodium. In an analogous fashion, after 75 min, the reaction of **7** with dppe provided the expected [Rh(PNSO)(dppe)] (**11**) as a major complex, along with smaller amounts of [Rh(dppe)₂] (**12**) and [Rh(PNSO)₂] (**6**) in a 16:4:1 ratio (Scheme 5). The reaction spectrum at 8 min (Figure 6) showed two species that disappeared over time: free ligand **3** (s, 60.0 ppm) and the [Rh(dppe)(COD)] complex **13** (d, 56.5 ppm, *J*_{Rh} = 149 Hz).²³ The reactivity of **7** with PPh₃ and dppe is consistent with **3** being a labile ligand. Thus, the PNSO ligand provided coordination sites for the incoming phosphine to

(23) de Wolf, E.; Spek, A. L.; Kuipers, B. W. M.; Philipse, A. P.; Meeldijk, J. D.; Bomans, P. H. H.; Frederik, P. M.; Deelman, B.; van Koten, G. *Tetrahedron* **2002**, *58*, 3911–3922.

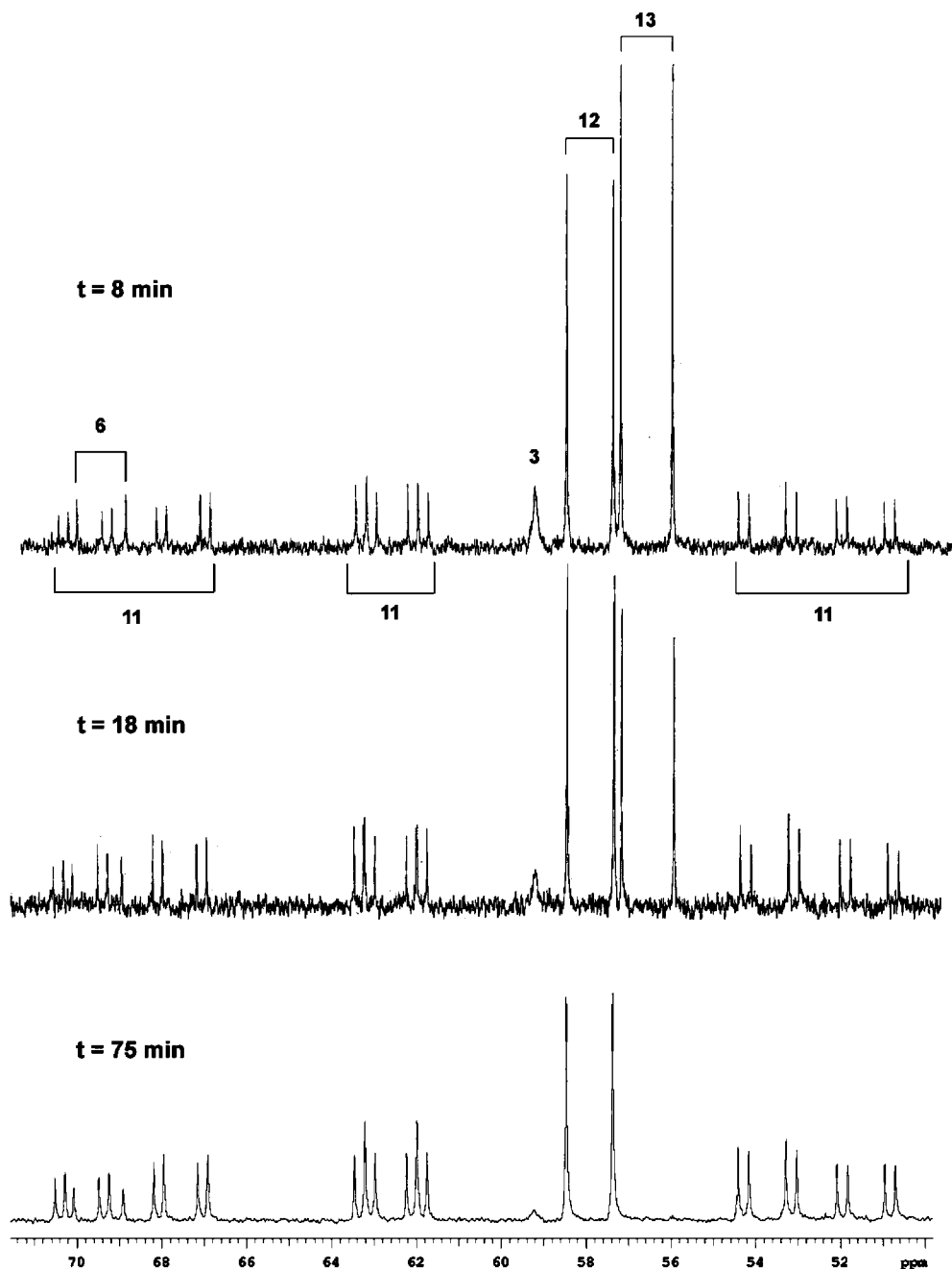


Figure 6. ^{31}P NMR monitoring for the reaction of complex **7** with 1 equiv of dppe in CDCl_3 .

coordinate the metal. This behavior allowed the displacement of the COD ligand with PPh_3 for **7**. It is known that the COD ligand cannot be displaced from $[\text{Rh}(\text{PPh}_3)_2(\text{COD})]$ complex with excess PPh_3 .²⁴ In addition, the emergence of $[\text{Rh}(\text{dppe})(\text{COD})]$ (**13**) and free PNSO ligand at the initial stages of the reaction reveals that dppe preferentially removes the PNSO rather than the COD ligand and that only later does the PNSO displace the COD ligand. With an electron-rich Rh^{I} center, the PNSO ligand in complexes **10** and **11** was presumed to display an S-coordination mode, in concordance with complexes in **6** and **8**.²⁵

Finally, interesting and distinct behaviors were observed when bis-PNSO complexes **6** and **9** were treated with PPh_3 and dppe (Scheme 5). Although **6** and **9** were similarly unreactive toward PPh_3 , they showed a different reaction profile with a diphosphine. Reaction of dppe with **6** produced a complete ligand exchange to yield the corresponding bis-dppe rhodium complex

12 in only 8 min. However, no reaction was observed after 5 h when cyclohexyl PNSO complex **9** was treated with dppe. The reactivity observed allows us to confirm that PNSO ligands are more competent ligands than monophosphines and that they cannot be replaced by PPh_3 . Furthermore, a chelating diphosphine such as dppe can easily replace the diphenylphosphino PNSO ligand **3** from the Rh coordination sphere, but not the cyclohexyl analog **4**.

Conclusions

Here, we report on the first rhodium (I) complexes with PNSO ligands. We have shown that these compounds can work as

(24) Albers, J.; Dinjus, E.; Pitter, S.; Walter, O. *J. Mol. Catal. A* **2004**, *219*, 41–46.

(25) No characteristic absorption bands were identified for the $\text{S}=\text{O}$ stretch in these complexes; see reference 14.

either P,O or P,S chelating ligands, depending on the electronic environment around the metal center. Thus, *N*-benzyl-*N*-diphenylphosphino-*tert*-butylsulfonamide (**3**) provides P,O coordination when olefin ligands (NBD or COD) are attached to the metal center. Alternatively, rhodium complexes with two PNSO ligands provides P,S coordination. [Rh(PNSO)₂] complexes preferentially show the thermodynamically most stable *cis* configuration. However, we have identified the kinetic *trans* complex with a dicyclohexylphosphino analog of **3**. Finally, ligand exchange experiments with PPh₃ and dppe show that PNSO ligands act as hemilabile ligands by providing coordination sites for the incoming phosphines.

Experimental Section

(+)-(R)-N-Benzyl-N-dicyclohexylphosphino-*tert*-butylsulfonamide Borane (4-BH₃). A 1.3 mL portion of *n*-BuLi 2.5 M in hexane (3.2 mmol) was added dropwise to a cooled (−78 °C) solution of the corresponding (*R*)-(−)-*N*-benzyl-*tert*-butylsulfonamide (600 mg, 2.8 mmol) in THF (20 mL). After 15 min, 0.72 mL (0.76 g, 3.3 mmol) of chlorodicyclohexylphosphine was added via syringe. The mixture was stirred at −78 °C for 1 h, and then the temperature was allowed to rise to −30 °C. At this point, 0.35 mL (0.28 g, 3.7 mmol) of BH₃–SMe₂ was added via syringe. The mixture was stirred at this temperature for 30 min and then warmed to 0 °C. The reaction was then quenched with 15 mL of water (caution: bubbling occurs) and extracted with Et₂O (30 mL). The organic layer was dried over MgSO₄, filtered, and concentrated under reduced pressure. The crude products were purified by flash column chromatography (SiO₂, hexanes/AcOEt, 80/20) to afford 1.00 g (85%) of the desired ligand as a foamy oil. [α]_D = +49.3 (*c* 1.0, CHCl₃). IR (KBr): ν_{max} 2932, 2853, 2390, 1451 cm^{−1}. ¹H NMR (400 MHz, CDCl₃): δ 0.20–0.80 (br s, 3H, BH₃), 1.10 (s, 9H), 1.14–1.38 (m, 6H), 1.50–1.98 (m, 11H), 2.00–2.24 (m, 5H), 4.46 (dd, *J* = 14 and 17 Hz, 1H), 4.68 (dd, *J* = 10 and 17 Hz, 1H), 7.21–7.38 (m, 5H). ¹³C NMR (100 MHz, CDCl₃): δ 24.2 (CH₃), 26.0–26.2 (m, 2 × CH₂), 26.9–27.3 (m, 4 × CH₂), 36.2 (d, *J*_P = 36 Hz, CH), 37.2 (d, *J*_P = 27 Hz, CH), 44.2 (d, *J*_P = 3 Hz, CH₂), 60.9 (C), 127.3 (CH), 128.2 (CH), 128.3 (CH), 139.0 (C) ppm. ³¹P NMR (121 MHz, CDCl₃): δ −63.9 (m) ppm. MS (CI, NH₃) *m/z* = 422 ([M + H]⁺, 25%), 421 ([M]⁺, 38%), 420 ([M − H]⁺, 100%), 364 ([M − C₄H₉]⁺, 21%). HRMS (ESI-TOF) calcd. for C₂₃H₄₁BNOPS: H, 420.2661; found, 420.2656.

(S_R)-[Rh(PNSO)(NBD)][TfO] (5**)**. Me₃SiOSO₂CF₃ (0.062 mL, 0.339 mmol) was added to a yellow solution of (nbd)Rh(acac) (0.1 g, 0.339 mmol) in dry THF (4 mL) under argon. The yellow-orange solution was stirred for 5 min, and (+)-**3** (0.134 g, 0.339 mmol) was then added in one portion. The solution briefly changed to orange, and a yellow precipitate separated to leave an orange liquor. The suspension was stirred at room temperature for 1 h and then added to vigorously stirred hexane (50 mL); a yellow-orange precipitate was formed. Most of the mother liquor was removed by canula and additional hexane (10 mL) was added. The precipitate was filtered off and dried to give a yellow solid (206 mg) as a mixture of complexes. Dark orange crystals of **5**, suitable for X-ray analysis, were obtained upon layering a THF solution of the resulting solid with Et₂O and hexane. IR (KBr): ν_{max} = 1260, 11173, 1035 cm^{−1}. ¹H NMR (400 MHz, CDCl₃): δ 1.34 (s, 9H), 1.62 (br 2), 3.99 (br, 2H), 4.42–4.48 (br m, 1H), 4.55–4.60 (br m, 1H), 6.83 (br, 2H), 7.16–7.20 (br, 4H), 7.42 (br, 3H), 7.51–7.60 (m, 8H), 7.82–7.86 (br, 3H) ppm. ³¹P NMR (121 MHz, CDCl₃): 115.8 (d, *J*_{Rh} = 193 Hz) ppm. MS (ESI, H₂O/CH₃CN (1:1) 1% formic) *m/z*: 893 [100, (2M − OTf − 2NBD)⁺], 590 [92, (M − OTf)⁺]. HRMS (ESI): calcd. for C₃₀H₃₄NOPSRh⁺, 590.1153; found, 590.1141.

(S_R)-*cis*-[Rh(PNSO)₂][TfO] (6**)**. [RhCl(COD)]₂ (0.1 g, 0.202 mmol) and AgOTf (0.104 g, 0.404 mmol) were placed in a Schlenk

flask protected from light with aluminum foil. The flask was then purged with N₂, and dry CH₂Cl₂ (2 mL) was added and stirred for 2 h. The resulting white precipitate (AgCl) was removed by filtration over Celite under nitrogen and subsequently washed with extra CH₂Cl₂ (3 × 2 mL). This orange solution was added dropwise into a Schlenk tube containing a solution of ligand (+)-**3** (0.320 g, 0.808 mmol) in CH₂Cl₂ (2 mL), and the mixture turned yellow. The reaction was stirred for 24 h at room temperature, then the yellow solution was evaporated under vacuum to a small volume (2–3 mL) and poured over vigorously stirred Et₂O (50 mL). The resulting precipitate was filtered, washed with 2 × 10 mL of Et₂O and dried to give complex **6** as a yellow shiny powder (0.36 g, 90%). Suitable crystals for X-ray analysis were obtained upon layering Et₂O over a CH₂Cl₂ solution of **6**. mp: 177 °C. [α]_D = +34 (*c* = 0.1, CHCl₃). IR (KBr): ν_{max} = 1439, 1272, 1149, 1131, 1106, 1062, 1031 cm^{−1}. ¹H NMR (400 MHz, CDCl₃): δ 1.47 (s, 18H), 4.35 (dd, *J* = 11 and 17 Hz, 2H), 4.43 (dd, *J* = 10 and 17 Hz, 2H), 6.66 (d, *J* = 8 Hz, 4H), 6.95–7.02 (m, 8H), 7.06–7.12 (m, 6H), 7.47–7.56 (m, 10H), 7.70 (t, *J* = 8 Hz, 2H) ppm. ¹³C NMR (100 MHz, {³¹P}, CDCl₃): δ 24.7 (3 × CH₃), 49.7 (CH₂), 68.6 (C), 125.5 (C), 128.0 (C), 128.3 (CH), 128.4 (CH), 128.7 (CH), 129.4 (CH), 130.0 (CH), 132.2 (CH), 132.6 (CH), 133.7 (C), 133.9 (CH), 134.2 (CH) ppm. ³¹P NMR (121 MHz, CDCl₃): 69.5 (d, *J* = 141 Hz) ppm. MS (ESI, H₂O/CH₃CN (1:1) 1% formic) *m/z*: 893 [100, (M − OTf)⁺]. HRMS (ESI): calcd. for C₄₆H₅₂N₂O₂P₂S₂Rh⁺, 893.1995; found, 893.1988. Anal. calcd. for C₄₇H₅₂F₃N₂O₅P₂RhS₂: C, 54.12; H, 5.03; N, 2.69. Found: C, 54.16; H, 4.93; N, 2.60.

(S_R)-[Rh(PNSO)(COD)][TfO] (7**)**. [RhCl(COD)]₂ (0.2 g, 0.404 mmol) and AgOTf (0.208 g, 0.809 mmol) were placed in a Schlenk flask protected from light with aluminum foil. The flask was then purged with N₂, and dry THF (2 mL) was added and stirred for 2 h. The resulting white precipitate (AgCl) was removed by filtration over Celite under nitrogen, and subsequently washed with extra THF (3 × 2 mL). The resulting orange solution was transferred into a Schlenk tube, and a solution of ligand **3** (0.320 g, 0.808 mmol) in THF was added dropwise. The reaction was stirred for 40 min at room temperature. Finally, the solvent was removed under vacuum to a small volume (2–3 mL), and Et₂O (10 mL) was layered over the reaction mixture. After one night, this afforded a crop of orange crystals (0.518 g, 85%) of complex **7**. Suitable yellow/orange crystals for X-ray analysis were obtained upon layering Et₂O over a CH₂Cl₂ solution of **7**. [α]_D = −115 (*c* = 0.1, CHCl₃). IR (KBr): ν_{max} = 1274, 1223, 1148, 1031 cm^{−1}. ¹H NMR (400 MHz, CDCl₃): δ 1.54 (s, 9H), 2.05–2.52 (br m, 8H), 3.55 (br, 1H), 3.74 (br, 1H), 4.49 (dd, *J* = 15 Hz and *J*_P = 4 Hz, 1H), 4.70 (dd, *J* = 15 Hz and *J*_P = 4 Hz, 1H), 5.37 (br, 1H), 5.68 (br, 1H), 6.69 (d, *J* = 7 Hz, 2H), 7.12–7.19 (m, 3H), 7.37 (br, t, *J* = 10 Hz, 2H), 7.57–7.71 (m, 6H), 8.01 (t, *J* = 8 Hz, 2H) ppm. ¹³C NMR (100 MHz, CDCl₃): δ 22.6 (3 × CH₃), 27.8 (CH₂), 28.4 (CH₂), 32.0 (CH₂), 33.5 (CH₂), 53.9 (CH₂), 61.9 (C), 70.4 (d, *J*_{Rh} = 14 Hz, CH), 73.8 (d, *J*_{Rh} = 14 Hz, CH), 105.6 (CH), 109.6 (CH), 127.0 (d, *J*_P = 56 Hz, C), 128.5 (C), 128.9 (C), 129.1 (CH), 130.0 (d, *J*_P = 10 Hz, CH), 130.2 (d, *J*_P = 11 Hz, CH), 130.5 (d, *J*_P = 11 Hz, CH), 131.2 (d, *J*_P = 56 Hz, C), 132.7 (d, *J*_P = 3 Hz, CH), 133.8 (CH), 134.4 (C), 135.5 (d, *J*_P = 16 Hz, CH) ppm. ³¹P NMR (121 MHz, CDCl₃): 116.5 (d, *J* = 167 Hz) ppm. MS (ESI, H₂O/CH₃CN (1:1) 1% formic) *m/z*: 893 [100, (2M − OTf − 2COD)⁺], 539 [37, (M + CH₃CN − COD)⁺]. HRMS (ESI): calcd. for C₂₄H₂₉N₂OPSRh⁺, 539.0787; found, 539.0786. Anal. calcd. for C₃₂H₃₈F₃NO₄PrhS₂: C, 50.86; H, 5.07; N, 1.85. Found C, 50.59; H, 4.90; N, 1.79.

(S_R)-*trans*-[Rh(PNSO)₂][TfO] (8**)**. Ligand 4-BH₃ (100 mg, 0.237 mmol, 2 equiv), DABCO (28 mg, 0.249 mmol, 2.1 equiv), and dry toluene (3 mL) were placed in a Schlenk tube under nitrogen. The solution was warmed to 70 °C for 4 h and then cooled to room temperature. In a separate Schlenk flask, [RhCl(COD)]₂ (29 mg, 0.059 mmol, 0.5 equiv), AgOTf (30 mg, 0.118 mmol, 1 equiv),

and dry THF (2 mL) were stirred at room temperature under nitrogen for 2 h. The resulting suspension was filtered over Celite under nitrogen. The Rh solution was then added to the ligand/DABCO mixture and allowed to stir for 24 h at room temperature. Removal of solvent under vacuum and purification by flash chromatography (acetone/hexanes, 60:40) afforded 116 mg (92%) of complex **8** as an air-stable yellowish solid. Suitable yellow/green crystals for X-ray analysis were obtained upon layering hexanes over a THF solution of **8**. $[\alpha]_D = -34$ ($c = 0.0016$, CHCl_3). IR (KBr): $\nu_{\text{max}} = 2931, 2854, 1450, 1264, 1141, 1057, 1028 \text{ cm}^{-1}$. ^1H NMR (400 MHz, CDCl_3): δ 0.93–1.38 (m, 18H), 1.46 (s, 18H), 1.73–1.86 (m, 18H), 2.06–2.06 (m, 2H), 2.11–2.20 (m, 4H), 2.36–2.48 (m, 2H), 4.29 (dt, $J = 6$ and 16 Hz, 2H), 4.46 (dt, $J = 4$ and 16 Hz, 2H), 7.35–7.46 (m, 10H) ppm. ^{13}C NMR (100 MHz, $\{^3\text{P}\}$, CDCl_3): δ 25.2 ($3 \times \text{CH}_3$), 25.59 (CH_2), 26.64 (CH_2), 26.3 (CH_2), 26.7 (CH_2), 27.4 (CH_2), 27.5 (CH_2), 27.9 (CH_2), 29.8 (CH_2), 30.6 (CH_2), 34.7 (CH), 39.5 (CH), 51.5 (CH_2), 69.5 (C), 128.8 (CH), 129.1 (CH), 129.2 (CH), 135.3 (C) ppm. ^{31}P NMR (121 MHz, CDCl_3): 86.2 (d, $J = 121$ Hz) ppm. MS (ESI, $\text{H}_2\text{O}/\text{CH}_3\text{CN}$ (1:1) 1% formic) m/z : 917.38 [59, ($\text{M} - \text{OTf})^+$], 121 [100%]. HRMS (ESI): calcd. for $\text{C}_{46}\text{H}_{76}\text{N}_2\text{O}_2\text{P}_2\text{S}_2\text{Rh}^+$, 917.3878; found, 917.3858.

(S_R)-*cis*-[Rh(PNSO) $_2$][TfO] (**9**). Solid complex **8** was suspended in dry THF under nitrogen and stirred overnight at room temperature. Solvent removal under vacuum afforded pure *cis*-Rh complex **9** as a yellow solid. Suitable crystals for X-ray analysis were obtained by layering hexanes over a solution of **9** in THF. $[\alpha]_D = -43$ ($c = 0.0021$, CHCl_3). IR (KBr): $\nu_{\text{max}} = 2931, 2854, 1450, 1267, 1151, 1123, 1031 \text{ cm}^{-1}$. ^1H NMR (400 MHz, CDCl_3): δ 0.82–1.26 (m, 16H), 1.63 (s, 18H), 1.70–1.81 (m, 20H), 1.96–2.03 (m, 2H), 2.15 (br, 2H), 2.33 (br, 2H), 4.41 (m, 4H), 7.35–7.42 (m, 6H), 7.445–7.48 (m, 4H) ppm. ^{13}C NMR (100 MHz, $\{^3\text{P}\}$, CDCl_3): δ 25.5 (CH_2), 25.72 (CH_2), 25.77 ($3 \times \text{CH}_3$), 26.0 (CH_2), 26.2 (CH_2), 27.0 (CH_2), 28.4 (CH_2), 29.9 (CH_2), 30.2 (CH_2), 35.3 (CH), 39.6 (CH), 51.6 (CH_2), 71.2 (C), 128.9 (CH), 129.2 (CH), 129.4 (CH), 135.1 (C) ppm. ^{31}P NMR (121 MHz, CDCl_3): 95.5 (d, $J = 135$ Hz) ppm. MS (ESI, $\text{H}_2\text{O}/\text{CH}_3\text{CN}$ (1:1) 1% formic) m/z : 918

[51, ($\text{MH} - \text{OTf})^+$], 917 [100, ($\text{M} - \text{OTf})^+$]. HRMS (ESI): calcd. for $\text{C}_{46}\text{H}_{76}\text{N}_2\text{O}_2\text{P}_2\text{S}_2\text{Rh}^+$, 917.3878; found, 917.3879. Anal. calcd. for $\text{C}_{47}\text{H}_{76}\text{F}_3\text{N}_2\text{O}_5\text{P}_2\text{RhS}_3 + 1/2\text{CH}_2\text{Cl}_2$: C, 51.41; H, 6.99; N, 2.52. Found: C, 51.34; H, 6.97; N, 2.53.

(S_R)-[Rh(PNSO)(PPh $_3$) $_2$][TfO] (**10**). A Schlenk tube containing complex **7** (0.05 g, 0.066 mmol), PPh $_3$ (0.034 g, 0.132 mmol) and dry dichloromethane was stirred under nitrogen for 1 h at room temperature. The resulting yellow-orange solution was poured over vigorously stirred hexane (50 mL), and the precipitate was filtered and washed with hexane (2×10 mL). The yellow solid was dried over high vacuum to provide 0.071 g (91%) of complex **10**. $[\alpha]_D = -16$ ($c = 0.1$, CHCl_3). IR (KBr): $\nu_{\text{max}} = 1436, 1272, 1148, 1093, 1031 \text{ cm}^{-1}$. ^1H NMR (400 MHz, CDCl_3): δ 1.12 (s, 9H), 4.05 (dd, $J = 17$ Hz and $J_P = 12$ Hz, 1H), 4.40 (dd, $J = 17$ Hz and $J_P = 12$ Hz, 1H), 6.40 (d, $J = 7$ Hz, 2H), 6.89–6.95 (m, 7H), 7.02–7.09 (m, 7H), 7.17–7.27 (m, overlap with CDCl_3 peak, 9H), 7.31–7.48 (m, 17H), 7.50–7.61 (m, 2H), 7.64–7.69 (m, 1H) ppm. ^{31}P NMR (121 MHz, CDCl_3): 23.7 (ddd, $J_{\text{PPcis}} = 37.2$, $J_{\text{PRh}} = 138.8$, $J_{\text{PPtrans}} = 279$ MHz), 32.2 (dt, $J_{\text{PPcis}} = 37.2$, $J_{\text{PRh}} = 155.8$), 63.6 (ddd, $J_{\text{PPcis}} = 37.3$, $J_{\text{PRh}} = 127.7$, $J_{\text{PPtrans}} = 278.9$ MHz) ppm. MS (ESI, $\text{H}_2\text{O}/\text{CH}_3\text{CN}$ (1:1) 1% formic) m/z : 760 [26, ($\text{M} - \text{PPh}_3$) $^+$], 801 [100], 1022 [8, ($\text{M})^+$]. HRMS (ESI): calcd. for $\text{C}_{59}\text{H}_{56}\text{NOP}_3\text{SRh}$, 1022.2345; found, 1022.2341.

Acknowledgment. We thank MEC (CTQ2005-623) and Enantia S. L. for financial support. T.A. thanks Enantia for financial support. We thank Prof. Anton Vidal-Ferran and Dr. Elisenda Reixach (ICIQ) for helpful assistance in ^{31}P decoupled NMR experiments.

Supporting Information Available: General methods and NMR spectra for ligand **4-BH $_3$** and complexes **6**, **7**, **8**, and **9**. X-ray crystal data with a complete numbering scheme, atomic distances and angles for **5**, **7**, **6**, and **8**. This material is available free of charge via the Internet at <http://pubs.acs.org>.

OM8006823